DEVELOPMENT OF A COUPLED HYDROLOGICAL-VEGETATION MODEL FOR A SMALL URBAN TROPICAL FRESHWATER WETLAND

MOHANADAS HARISH CHANDAR

DEPARTMENT OF CIVIL AND ENVIRONMENTAL ENGINEERING

NATIONAL UNIVERSITY OF SINGAPORE

2010/2011

DEVELOPMENT OF A COUPLED HYDROLOGICAL-VEGETATION MODEL FOR A SMALL URBAN TROPICAL FRESHWATER WETLAND

MOHANADAS HARISH CHANDAR

A THESIS SUBMITTED

FOR THE DEGREE OF BACHELOR OF ENGINEERING

DEPARTMENT OF CIVIL AND ENVIRONMENTAL ENGINEERING

NATIONAL UNIVERSITY OF SINGAPORE

Acknowledgments

I am grateful, foremost to my supervisor, Assistant Professor Chui Ting Fong May, for her support and guidance from the beginning till the end of my final year project. I am deeply touched by the freedom she allowed me in developing the project according to my interests, while keeping me focused on the objectives of the project itself.

I also grateful to Professor Poon Kok Kwang for introducing me to the field of numerical modeling. His introductory lectures covering the pitfalls and challenges in numerical modeling set the stage for much of my final year project. Any errors and shortfalls are however solely mine.

Ms Lim Chi Cheng Christina and Madam Sarimah Bte Mustafa provided excellent administrative support throughout the duration of my final year project, and throughout the duration of my undergraduate life in the Department of Civil and Environmental Engineering.

Special thanks go to Professor Somsak Swaddiwudhipong for being instrumental in developing my love and enthusiasm for civil and environmental engineering, and for graciously supporting my pursuits in self-directed learning.

Last but not least, I wish to thank my examiner, Dr Liong Shie-Yui, for taking the time and effort in critiquing both this thesis and the oral presentations for my final year project.

Table of Contents

Summary

A coupled hydrological-vegetation model was developed for the Nee Soon Wetland—a small freshwater wetland located within the dense urbanised island state of Singapore. The wetland forms a significant part of the Central Catchment Area of the island—an area containing several of its most important forests and reservoirs, and home to several rare and endangered species of terrestrial and aquatic wildlife and vegetation. The model incorporates groundwater dynamics of the phreatic and vadose zones, and vegetation dynamics of three vegetation species (a flood resistant wetland species, a less flood resistant wetland species, and a dryland species). It also incorporates terrain relief and land-use information, and stochastically generated rainfall data. The coupled nature of the model allows it to account for the effects of hydrology and vegetation on one another. This is especially useful for wetlands, as wetland hydrology and wetland ecology are intrinsically bound to one another. The hydrological regime is well established to be the dominant forcing function for wetland ecology, while evapotranspiration from vegetation is commonly the dominant sink for wetland hydrology. The spatial terrain relief and land-use inputs allow for investigation of vegetation patterning, and the effect of urban developments on the wetland itself. The temporal rainfall inputs allow the development of the wetland to be tracked over time. The model has direct application for quantitative study and management of the Nee Soon Wetland itself, and given sufficient ground and rainfall information, can be adapted for quantitative study and management of wetlands worldwide.

List of Figures

List of Tables

Chapter 1

Introduction

The Nee Soon Wetland (also called Nee Soon Swamp Forest or Nee Soon Freshwater Swamp) is a small tropical freshwater wetland located within the heart of the dense, urbanized, island-state of Singapore (see Figure 1.1 and Figure 1.2). The wetland is located within the Central Catchment Area of the island—an area containing several of the island's most important forests and reservoirs, and also home to several rare and endangered and species of fish, amphibians, reptiles, birds and mammals (Ng and Lim 1992).

Challenges As is common in other areas of the world, much of the original wetland areas in Singapore have been drained or filled to make way for urban development. The Nee Soon Wetland is now the last relatively intact major area of freshwater swamp forest in Singapore (Ng and Lim 1992). Fortunately, in recent years, there has been a renewed interest towards the conservation of wetlands in Singapore, resulting in the legislation of the wetland and its surrounding forests as the Central Catchment Nature Reserve. The Nee Soon Wetland however, is still faced with conservation challenges, due to its small size and close proximity to dense urban areas. Nearby construction and new urban developments have the potential to affect the wetland hydrological regime and wetland ecology, both directly and indirectly.

In studying wetland ecosystems, a further challenge arises from the strong in-

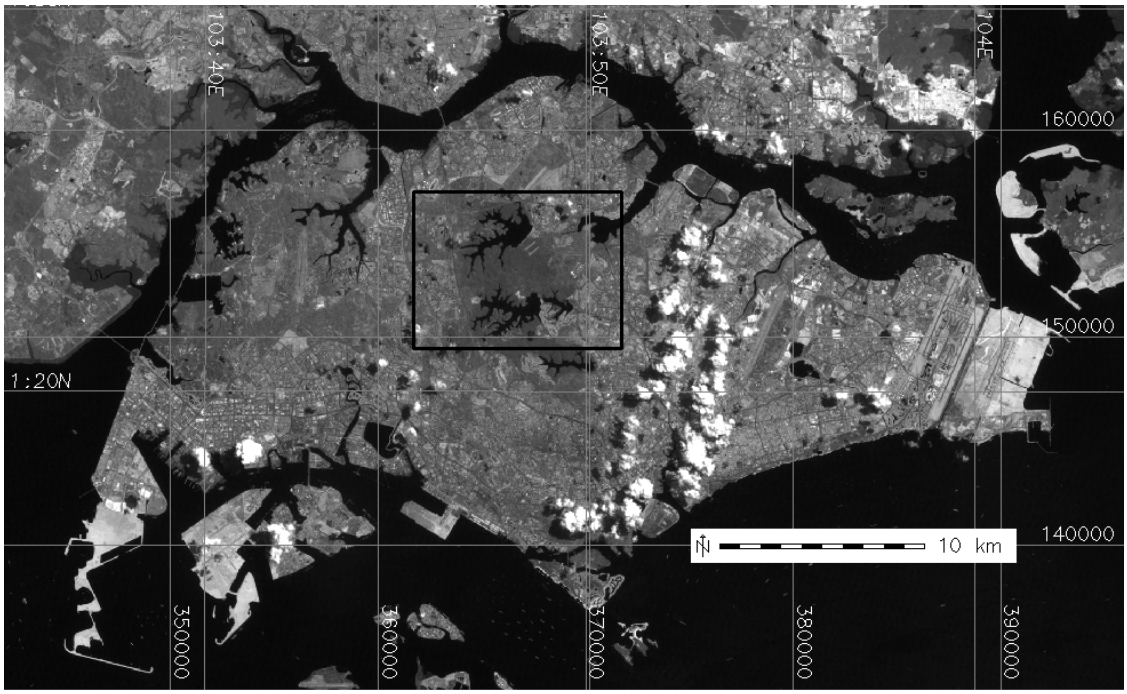

Figure 1.1: Image of Singapore from the Landsat 5 satellite (band 5—mid infrared image). The Nee Soon Wetland is located within the forested region of the boxed outline (see Figure 1.2 for an enlarged image.) Satellite image courtesy of U.S. Geological Survey.

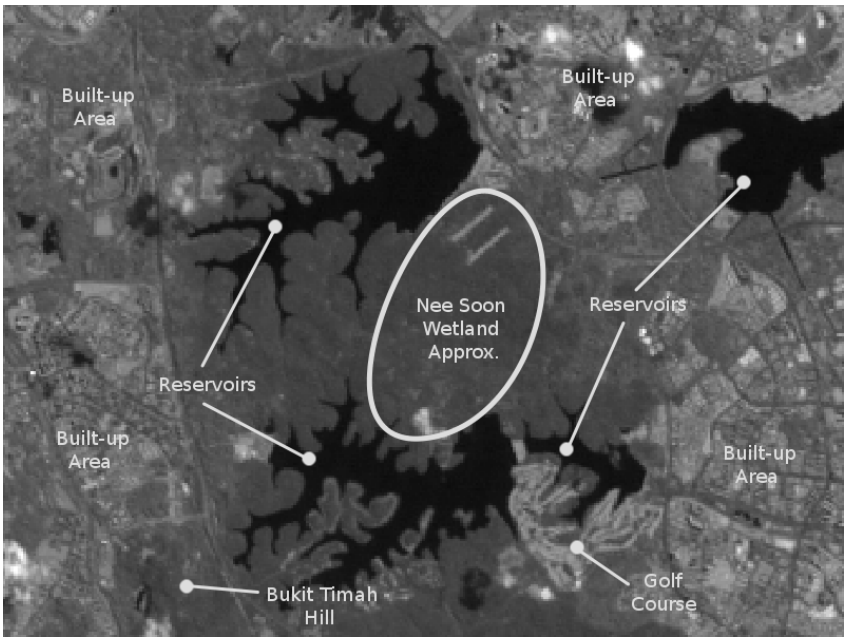

Figure 1.2: Enlargement of the boxed outline from Figure 1.1, showing the approximate location of the Nee Soon Wetland and its surrounding land-use characteristics. The large, black areas are reservoirs. Moist areas, such as forests and vegetation patches, are medium grey. Built-up areas, golf courses and bare soil appear light grey.

fluence of wetland hydrology and wetland vegetation on one another. It is well established by ecologists that the hydrological regime of a wetland is the dominant forcing function for wetland ecology (Keddy 2000). It is also well known by hydrologists that evapotranspiration from vegetation is the major sink in most wetlands, and that evapotranspiration can vary significantly from one plant species to another (Hunt and Wilcox 2003). Due to the strong influence of wetland hydrology and wetland vegetation on one another, quantitative studies and models of wetlands are likely to require the coupling of both hydrological and vegetation dynamics. Such studies are are however hampered as hydrologists and ecologists are commonly unfamiliar with the relevant aspects of one another's fields (Wassen and Grootjans 1996; Hunt and Wilcox 2003).

Opportunities. Ecohydrology presents a relatively new interdisciplinary paradigm, directed at fundamental process understanding of the bidirectional interactions and feedback mechanisms between hydrology and biota, in a variety of ecosystems, and over a range of spatial and temporal scales (Hannah, Wood, and Sadler 2004). It shows promise in quantitatively linking hydrological and vegetation dynamics.

Another development has been the explosion in the amount of information and computing power available to researchers. Remotely sensed topographical, vegetation and land-use information of almost the entire earth is publicly available at a variety of spatial, temporal and radiometric scales and resolutions (see Lillesand, Kiefer, and Chipman (2003) for an introduction). Multi-core end-user laptop computers can now solve complicated coupled numerical problems within reasonable amounts of time, and software for the quick and easy visualization of results is widely available.

Engineers, due to their technical and problem solving background, are well poised to tap onto these new developments. Together with scientists and managers, they can utilise them in solving interdisciplinary challenges, such as those related to the Nee Soon Wetland.

Final year project. For my final year project, I have attempted to tap upon the above opportunities, and develop a coupled hydrological-vegetation model of the Nee Soon Wetland, under the supervision of Assistant Professor Chui Ting Fong May. The resulting model combines remotely sensed terrain relief and land-use information, with concepts and models from the fields of hydrology, mathematical biology, ecology and ecohydrology. It also provides a suitably georeferenced, two dimensional (2D) aerial representation of the wetland, and incorporates time varying, stochastically generated rainfall patterns.

By coupling hydrological and vegetation dynamics, the model addresses the challenge of accounting for the effects of wetland hydrology and vegetation on one another. By incorporating terrain relief and land-use information, it accounts for vegetation patterning and hydrological conditions induced by the terrain itself, and addresses the close proximity of the Nee Soon Wetland to differing land-uses. The georeferenced, 2D aerial representation of the wetland allows results to be presented in a form that is informative and factual, yet easily understandable by both experts and non-experts.

The model has direct application for quantitative study and management of the Nee Soon Wetland itself. Given sufficient field ground and rainfall information, it can also be adapted for quantitative study and management of wetlands worldwide.

1.1 Objectives and Scope

The current study aims to develop a coupled hydrological-vegetation model for the Nee Soon Wetland. The model is to provide suitably georeferenced 2D aerial representation of the wetland and the hydrological-vegetation interactions within it. The scope of the model is limited to explicitly modeling

- Groundwater dynamics in both the vadose and phreatic zones, and
- Biomass dynamics of three hypothetical plant species (a flood resistant wetland species, a less flood resistant wetland species, and a dryland species)

Chapter 2

Background

A background study was undertaken by reviewing the literature in wetland ecology, mathematical modeling, ecohydrological models, and species permanence in competitive Lotka-Volterra systems. Concepts and information gathered were subsequently used in creation and evaluation of the model. This chapter highlights some of the concepts and information gathered.

2.1 Wetland Ecology

From an ecological perspective, wetlands have three critical characteristics: temporary or permanent inundation by water, soil dominated by anaerobic processes due to anoxic soil conditions, and vegetation that is adapted particularly to tolerate such conditions (Keddy 2000, pp. 3–7).

The temporary or permanent inundation of water causes wetland soils to become saturated, meaning that pore spaces in soil that would have been occupied by air, and thus oxygen, are filled up with water instead. Diffusion of gases through water is about 10,000 times slower than diffusion through air, leading to low levels of oxygen in soil, insufficient for soil biota to maintain aerobic respiration (Richardson, Arndt, and Montgomery 2001).

While green plants produce more oxygen than they use during daylight hours,

oxygen produced by plants during photosynthesis quickly diffuses away, and very little of it is transported to the root tips (Cronk and Fennessy 2001). Due to the low levels of oxygen in wetland soils, plant roots undergo anaerobic respiration, significantly reducing the amount of energy produced.

Wetland plants can either tolerate long periods of anaerobic respiration or have evolved other adaptations such as internal gas-transport systems, root system modifications such as adventitious, shallow or erect roots, and carbohydrate storage organs (Cronk and Fennessy 2001).

Classification A large variety of wetland classification systems exist (see Keddy (2000, chap. 2)), but on a basic level, wetlands can be classified into six basic types: swamp, marsh, bog, fen, wet meadow and aquatic (Keddy 2000, pp. 18–19). Keddy (2000) describes the above wetland types. Swamps and marshes are formed in locations of hydric soils while bogs and fens are formed in locations of peat. Swamps are dominated by trees while marshes are dominated by herbaceous plants. Vegetation in bogs is rooted in deep peat while vegetation in fens is rooted in shallow peat. Wet meadows are characterised by temporary episodes of flooding, preventing the growth of terrestrial or swamp plants, but during can be colonised by plant communities typical of moist soils during dry periods. Aquatic environments are covered by at least 25 cm of water and are dominated by aquatic plants.

Wetland Dynamics From the perspective of wetland dynamics, four wetland types—swamp, wet meadow, marsh and aquatic—represent a continuum resulting from the presence of wetland vegetation types associated with an increasing duration of flooding (Keddy 2000, p. 189). Woody plants (swamp) are particularly sensitive to flooding, and in long durations of flooding (about 0.3 to 3 years) are replaced by herbaceous plants (wet meadow and marsh). Herbaceous plants are themselves replaced by aquatic plants (aquatic) under situations of continuous flooding, as herbaceous plants usually require occasional dry periods for regeneration from seeds

(Keddy 2000, p. 190–192).

Wetland dynamics is thus largely controlled by the hydrological regime of the wetland, especially the magnitude and frequency (seasonal and over several years) of water level fluctuations (Keddy 2000, p. 178). Water level fluctuations can be both seasonal and stretched out over periods of years or decades. Water level fluctuations are a common occurance in rivers and watersheds, and lakes, resulting in a patterns of vegetation zonation, from those typically found in aquatic habitats to those in swamp habitats (Keddy 2000, pp. 194–208).

2.2 Mathematical Modeling

Barbour and Krahn (2004) state that numerical modeling in engineering is often used for interpretation of field data and for comparison between design alternatives. They go on to state that at times, models can also be used for prediction of field behaviour, but this is very difficult to achieve. In either case, numerical modeling involves continual verification of the model with field data, and continual calibration and improvements after verification. They recommended starting off model development with simple models and increasing complexity iteratively and only when needed.

2.3 Coupled Hydrological-Vegetation Models

Coupled hydrological-vegetation models in the literature were reviewed. In general, vegetation dynamics was coupled to either water table depth or soil moisture within root zone or both, and hydrological dynamics was coupled to evapotranspiration.

Loheide II and Gorelick (2007) presented an example of a largely empirical model simulating equilibrium conditions. Water table depth was empirically related to relative equilibrium proportions of two different kinds of vegetation: one wetland and one dryland. To cater for seasonally varying water table depth, water table

depth at 3 different times of the year were considered—corresponding to periods of vegetation growth, vegetation decay, and initiation of vegetation growth.

Muneepeerakul et al. (2008) presented an example of a largely mechanistic and transient model. Growth rate was mechanistically related to water table depth and average soil moisture within root zone. Carrying capacity was semi-empirically related to water table depth. Competition between two species of wetland vegetation was also mechanistically modeled using a two-species competitive Lotka-Volterra system. Stochastically varying rainfall exerted a strong but delayed influence on biomass density.

The largely mechanistic models were more complex than largely empirical ones, but could provide better explanations for the underlying physical phenomena. The largely empirical models had the virtue of being simpler and easier to use and verify.

2.4 Competitive Lotka-Volterra Systems and Species Permanence

The competition dynamics of multiple competing species of vegetation within a single habitat can be described by the competitive Lotka-Volterra system. The two-dimensional form of the competitive Lotka-Volterra system involves two competing species, denoted by x and y, with populations N_x and N_y. In the absence of both intra- and inter-species competition, per capita growth rates, $\frac{\dot{N}_x}{N_x}$ and $\frac{\dot{N}_y}{N_y}$, are assumed constant at the values r_x and r_y. In the presence of competition, the per-capita growth rates are reduced linearly in relation to the populations of both intra- and inter-species competitors. The strength of the competition is expressed by the positive constants a_{xx}, a_{xy}, a_{yx} and a_{yy}, resulting in the two-species competitive Lotka-Volterra system:

$$\frac{\dot{N}_x}{N_y} = r_x - a_{xx}N_x - a_{xy}N_y, \quad \frac{\dot{N}_x}{N_y} = r_y - a_{yx}N_x - a_{yy}N_y. \tag{2.1}$$

From the point of view of environmental or ecological management, it is often desirable to allow nature to take its course, while ensuring the permanence of all species in the ecosystem. At other times, such as when intending to eradicate weeds or invasive species, it may be preferable to completely eradicate a species completely.

Under the above two-species competitive Lotka-Volterra system, a situation of coexistence of both species in the long-run (species permanence) is achieved when intra-species competition is greater than inter-species competition, i.e. $a_{xx}a_{yy} > a_{xy}a_{yx}$, (Farkas 2001, p. 31). Given that $a_{xx}a_{yy} \neq a_{xy}a_{yx}$, three other types of permanence characteristics can be derived as well (Farkas 2001, pp. 30–32). Including the above case of coexistence of both species in the long run, the permanence characteristics of the two-species competitive Lotka-Volterra system are

1. Coexistence of both species: $a_{xx}a_{yy} > a_{xy}a_{yx}$ (intra-species competition is stronger)

2. Species x dies out: $r_x a_{yy} < r_y a_{xy}$ and $r_x a_{yx} < r_y a_{xx}$

3. Species y dies out: $r_y a_{xx} < r_x a_{yx}$ and $r_y a_{xy} < r_x a_{yy}$

4. Either species dies out, depending on initial conditions: $\frac{a_{xx}}{a_{yx}} < \frac{r_x}{r_y} < \frac{a_{xy}}{a_{yy}}$

The competitive Lotka-Volterra systems used in ecohydrological models such as Muneepeerakul et al. (2008), are more complex, with growth rates and competitive strengths varying with hydrological conditions. Thus, while it may be tempting to extend the above results to analysis of such more complex competitive Lotka-Volterra systems, it is important to note that the results may only be applicable in describing the short-term behaviour of the system, rather than its long-term behaviour.

Chapter 3

Materials and Methods

The coupled hydrological-vegetation model was implemented within a finite element, partial differential equation (PDE) solver called COMSOL Multiphysics (COMSOL AB. 2010). A two-dimensional (2D) domain, covering the entire land surface of mainland Singapore was used (see Figure 3.1). A fairly accurate spatial representation of the Nee Soon Wetland was derived from satellite photos and digital elevation models using the software programs GRASS GIS (GRASS Development Team 2008) and QCAD (RibbonSoft GmbH 2008). Spatial coordinates on the domain could be approximately georeferenced to the Universal Transverse Mercator (UTM) map projection. Closer to the area of interest, features were georeferenced more accurately ($1\,\mathrm{km} \rightarrow 100\,\mathrm{m} \rightarrow 10\,\mathrm{m}$), and the finite element grid was made finer.

The model was made up of the following components: hydrological dynamics, vegetation dynamics, coupling relationships between hydrology and vegetation, spatial inputs, and temporal inputs. The finest timescale it could be interpreted at was the daily timescale, as intra-day variations in evapotranspiration and rainfall were not considered.

The remainder of this chapter first describes each component of the model, after which, the mathematical details of the model are presented.

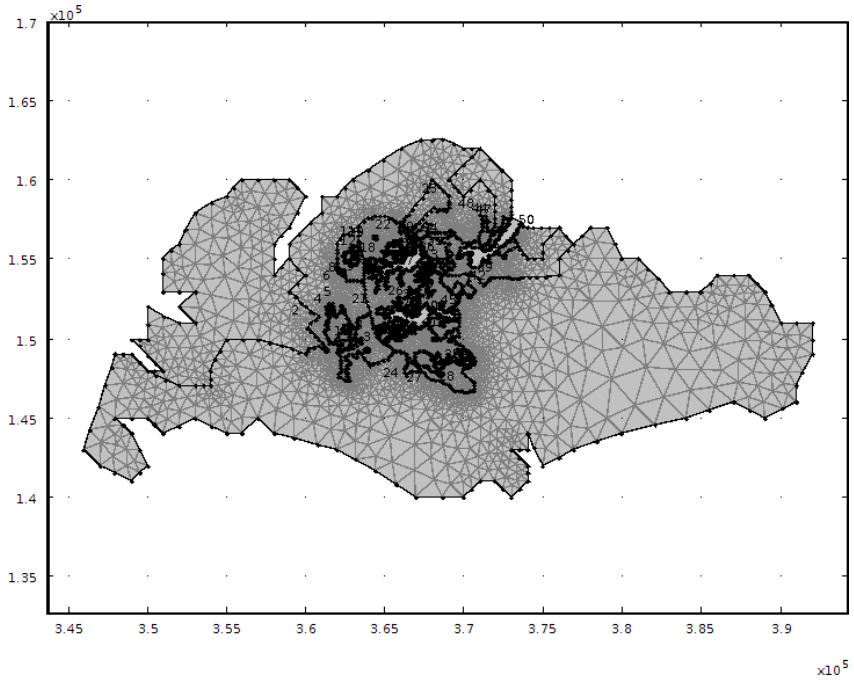

Figure 3.1: Model with finite element grid as implemented in COMSOL Multiphysics. Coordinates are from the Universal Transverse Mercator (UTM) projection.

3.1 Model Description

Hydrological dynamics. Hydrological dynamics in the model was separated into dynamics of a phreatic zone (saturated soil, below the water table) and dynamics of a vadose zone (unsaturated soil, above the water table). The phreatic zone was modeled as a two-dimensional unconfined aquifer in the horizontal plane, being recharged by the overlying vadose zone. The vadose zone was modeled as a mass balance at each point on the horizontal plane. It was characterised by depth-averaged relative soil saturation, infiltration at the soil surface, and leakage into the underlying phreatic zone. In addition, evapotranspiration from vegetation functioned as a dynamically varying hydrological sink for both the phreatic and vadose zones.

Vegetation dynamics. Vegetation dynamics in the model was represented by a three-species competitive Lotka-Volterra system. The three species corresponded to a flood resistant wetland species (species 1), a less flood resistant wetland species (species 2) and a dryland species (species 3). Growth rates were dependent upon evapotranspiration from both the phreatic and vadose zones. Carrying capacities

were dependent upon water table depth. The dryland species was taken to be mesophytic—adapted to extracting water from the vadose zone. The two wetland species were adapted to extracting water from the phreatic zone instead.

Coupling relationships between hydrology and vegetation. The coupling relationships between hydrology and vegetation were largely adapted from the paper by Muneepeerakul et al. (2008). Evapotranspiration from both the phreatic and vadose zones determined the growth rate of each species, while also functioning as a hydrological sink. Conversely, evapotranspiration was modulated by water table depth and relative soil saturation of the vadose zone. As a greater portion of plant roots became submerged under the water table, anoxic stress set in due to waterlogging, reducing the plant's ability to evapotranspire, hence reducing evapotranspiration itself. Also, as relative soil saturation decreased below a certain threshold, plant water stress due to soil dryness set in, reducing the plant's ability to evapotranspire. This again lead to reduced evapotranspiration. Through the above mechanisms, and through linking vegetation growth rates to evapotranspiration, and carrying capacities to water table depth, hydrological and vegetation dynamics were coupled with one another.

Spatial inputs. Spatial inputs to the model comprised of terrain information and land-use characteristics. Terrain information consisted of elevation data through a digital elevation model (DEM) and location of streams within the Nee Soon Wetland. The DEM of the island of Singapore was from the Shuttle Radar Topography Mission (SRTM), and had been further processed by Jarvis et al. (2008). Bilinear interpolation was used to determine the elevation at any point within the domain of the model. Streams were modeled as zero-width interior boundaries, and were assigned Dirichlet boundary conditions representing the elevation of their water surface.

Land-use was classified into reservoirs and lakes, built-up areas, vegetated areas,

and golf courses (see Figure 3.2). The different land-use classes were modeled differently. Reservoirs and lakes were not modeled directly and were cut-out from the domain of the model. Instead, the boundaries of reservoirs and lakes were assigned Dirichlet boundary conditions representing the elevation of their water surface. Water surface elevation of the lakes and reservoirs was retrieved from the SRTM DEM (Jarvis et al. 2008) as well. Built-up areas were assumed to contain no vegetation and to have zero infiltration from rainfall. Vegetated areas and golf courses both contained vegetation and were allowed infiltration if the water table was below the ground surface. In golf courses however, the vegetation composition was assumed to be artificially held constant.

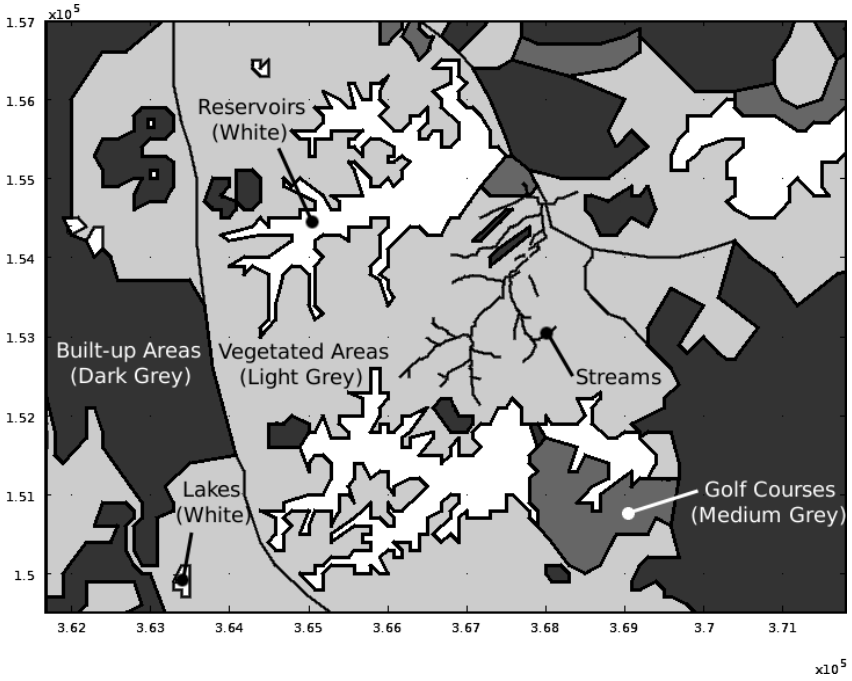

Figure 3.2: Land-use classification used in the model: reservoirs are lakes are white, built-up areas are dark grey, vegetated areas are light grey, and golf courses are medium grey. Coordinates are from the Universal Transverse Mercator (UTM) projection.

Temporal inputs. Temporal inputs to the model consisted of a stochastically varying rainfall pattern. For simplicity, rainfall was taken to be uniform over the entire domain. Rainfall events were modeled as a binomial process, with each day representing one binomial event. This was appropriate for the model as the daily timescale was the finest timescale it could be interpreted at. Values for the amount

of rainfall during a rainfall event were assumed to follow a geometric distribution.

Rainfall was assumed to fall at a constant rate over the entire day. This approximation was valid for all but the most intense rainstorms. Firstly, the raindrop arrival rate of most rainstorms was less than the maximum leakage rate from the vadose zone into the phreatic zone. Secondly, in nature, infiltration capacity at the beginning of a rainstorm is considerably higher than the subsequent fairly constant infiltration capacity (Brady and Weil 2008). This natural phenomenon additionally allowed for infiltration from short durations of extremely intense rainfall to be adequately modeled as well.

Realised values for rainfall events and amount of rainfall during rainfall events were pre-generated using a spreadsheet, and input into the model before the start of model runs.

3.2 Phreatic Zone Dynamics

3.2.1 Groundwater flow

Groundwater flow within the phreatic zone was modeled as saturated groundwater flow within a two-dimensional (2D) unconfined aquifer in the horizontal plane. Hydraulic head, H [L], was depth averaged and taken relative to a datum at sea level, i.e. zero elevation. It was given by

$$s_y \frac{\partial H}{\partial t} - K_s \left[\frac{\partial}{\partial x} \left(b \frac{\partial H}{\partial x} \right) + \frac{\partial}{\partial y} \left(b \frac{\partial H}{\partial y} \right) \right] = Re - q_{Ts} - q_E \qquad (3.1)$$

where S_y [$-$] is the specific yield; H [L] is the depth averaged hydraulic head, taken relative to a datum at sea level, i.e. zero elevation; b [L] is the saturated thickness; Re [LT^{-1}] represents recharge of the phreatic zone; q_{Ts} [LT^{-1}] is the total evapotranspiration per unit land area from the phreatic zone; and q_E [LT^{-1}] represents exfiltration, which occurs when the water table rises above the ground surface.

Dirichlet boundary conditions for H were set on all reservoir and lake boundaries. The value of H was taken to be equal to their water surface elevation. Water surface elevation was derived from the SRTM DEM (Jarvis et al. 2008).

Streams were taken to be zero-width interior boundaries. For simplicity, streams were assumed to be 1 m in depth, and a Dirichlet condition of $H = E_{grd} + 1$ was set on all stream boundaries, where E_{grd} [L] was the elevation of the ground surface.

Coastal boundaries were set to $H = 0$.

Specific yield. Specific yield was coupled to the vadose zone dynamics using a simple relationship. It was taken to be given by

$$s_y = \eta\,(1 - S) \tag{3.2}$$

where η [$-$] is soil porosity; and S [$-$] is the relative soil saturation of the vadose zone.

Saturated thickness. In the model, a level impermeable layer was assumed. Saturated thickness, b [L], was therefore given by

$$b = H - E_{bot} \tag{3.3}$$

where E_{bot} [L] is the elevation of the level impermeable layer, positive if above sea level, and negative if below sea level.

3.2.2 Recharge

Recharge of the phreatic zone, Re [LT^{-1}], was taken to be equal to leakage from the vadose zone, i.e.

$$Re = Le. \tag{3.4}$$

where Le [LT^{-1}] represented leakage from the vadose zone into the phreatic zone.

3.2.3 Exfiltration

Exfiltration of water from the phreatic zone was a term included to represent the removal of water when the water table rose above the soil surface, i.e. when flooding occurred. The water removed was assumed to have first flown into the streams through overland flow, and then into the sea through streamflow. In the current model, overland flow and streamflow were not directly modeled. Instead, a calibration factor was included within the exfiltration term to control the size of flooded areas. Exfiltration, q_E [LT^{-1}], was modeled as a depth-dependent flux:

$$q_E = \begin{cases} -wN, & w < 0, \\ 0, & w \geq 0, \end{cases} \tag{3.5}$$

where N [T^{-1}] is the exfiltration calibration factor, based on ground observations of flooding; and w [L] is the water table depth, measured from the ground surface downwards, with negative values indicating flooding.

Water table depth. Water table depth was measured from the ground surface downwards. Thus, negative values for water table depth represented flooding. As hydraulic head, H, was taken relative to sea level, water table depth, w [L], was given by

$$w = E_{grd} - H \tag{3.6}$$

where E_{grd} [L] refers to the elevation of the ground surface.

3.3 Vadose Zone Dynamics

3.3.1 Relative soil saturation

Relative soil saturation within the vadose zone was modeled using a mass balance at each point on a horizontal 2D plane. Only vertical flows were considered, similar to the case in Rodriguez-Iturbe et al. (1999), Rodriguez-Iturbe et al. (2001) and Laio et al. (2001). This gives a value for the relative soil saturation that is depth-averaged over the entire depth of the vadose zone. The equation used for modeling depth-averaged relative soil saturation within the vadose zone, S [$-$], was

$$\frac{\partial S}{\partial t} = \begin{cases} -(S - S_{fc}), & w \leq 0, \\ \frac{1}{\eta w}(I - q_{Tuns} - Le), & w > 0, \end{cases} \tag{3.7}$$

where S_{fc} [$-$] is relative soil saturation at field capacity; I [LT^{-1}] is the rate of infiltration from rainfall; q_{Tuns} [LT^{-1}] is the total evapotranspiration per unit land area from the vadose zone; and Le [LT^{-1}] is the rate of leakage from the vadose zone into the phreatic zone.

3.3.2 Infiltration

Infiltration was modeled according to the land-use classification. Built-up areas were assumed to have zero infiltration from rainfall. In vegetated areas and in golf courses, all rainfall was taken to infiltrate into the soil, unless the water table was above the ground surface. Infiltration ceased when the water table was above the ground surface. Infiltration, I [LT^{-1}], was thus given by

$$I = \begin{cases} 0, & w \leq 0, \\ Ra, & w > 0. \end{cases} \tag{3.8}$$

where Ra [LT^{-1}] is the rate of raindrop arrival per unit surface area.

3.3.3 Leakage

Leakage from the vadose zone into the phreatic zone was taken to be zero at and below field capacity and to have a maximum value equal to the saturated hydraulic conductivity, K_s, when the soil becomes fully saturated. This corresponds to the common assumption of a unit hydraulic gradient. For values of relative soil saturation between field capacity and complete saturation, leakage was assumed to increase linearly with relative soil saturation, as was done in Rodriguez-Iturbe et al. (1999). Leakage, Le [LT^{-1}], was thus modeled as

$$Le = \begin{cases} 0, & 0 \leq S \leq S_{fc}, \\ K_s \dfrac{S - S_{fc}}{1 - S_{fc}}, & S_{fc} < S \leq 1, \end{cases} \tag{3.9}$$

where S_{fc} [$-$] is the soil field capacity—the point at which further water loss due to gravity is negligible; and K_s [LT^{-1}] is the saturated hydraulic conductivity of the soil.

3.4 Vegetation Dynamics

3.4.1 Vegetation biomass

Vegetation biomass of the 3 species was determined through a competitive Lotka-Volterra system. Species 1 corresponded to a flood resistant wetland species, species 2 to a less flood resistant wetland species and species 3 to a dryland species. Biomass per unit land area of each species i, B_i [ML^{-2}], is given by

$$\frac{\partial B_i}{\partial t} = B_i(r_i - a_{ii}B_i - \sum_{i \neq j} a_{ij}B_j - \beta_i) \tag{3.10}$$

where r_i [T^{-1}] represents the growth rate of species i; a_{ii} [$-$] represents the strength of intra-species competition; a_{ij} [$-$] represents the strength of inter-species competition; and β_i [T^{-1}] is the biomass decay rate.

Strength of intra- and inter-species competition. Strength of intra- and inter-species competition, a_{ij} [−], was dependent upon effective growth rate, carrying capacity and impact coefficients between species. It was given by

$$a_{ij} = \alpha_{ij} \frac{r_i}{K_i} \tag{3.11}$$

where α_{ij} [−] is the impact coefficient of species j on species i; and K_i [ML^{-2}] represents the carrying capacity of species i.

3.4.2 Growth rate

Growth rate, r_i [T^{-1}], was linked to evapotranspiration from both the phreatic and vadose zones, using the relationships proposed in Muneepeerakul et al. (2008). An equivalent form of the above relationships is given by

$$r_i = \frac{\omega_i}{B_i}(q_{Tsi} + q_{Tunsi}) \tag{3.12}$$

where ω_i [ML^{-3}] denotes intrinsic water use efficiency; q_{Tsi} [LT^{-1}] denotes evapotranspiration per unit land area from the phreatic zone for species i; and q_{Tunsi} [LT^{-1}] represents evapotranspiration per unit land area from the vadose zone for species i.

3.4.3 Carrying capacity

Carrying capacity of all species was modeled upon the framework proposed by Ridolfi, D'Odorico, and Laio (2006). The two wetland species were assumed to be adapted to extracting water from both the vadose and phreatic zones. Species 1 was most adapted to water table depths very near the ground surface while species 2 was most adapted to slightly deeper water table depths. The dryland species was assumed to be mesophytic—adapted to extracting water from the vadose zone, and not requiring uptake from the phreatic zone. It was ill-suited to water table depths near the ground surface. The carrying capacity curves for the three species are given in Figure 3.3.

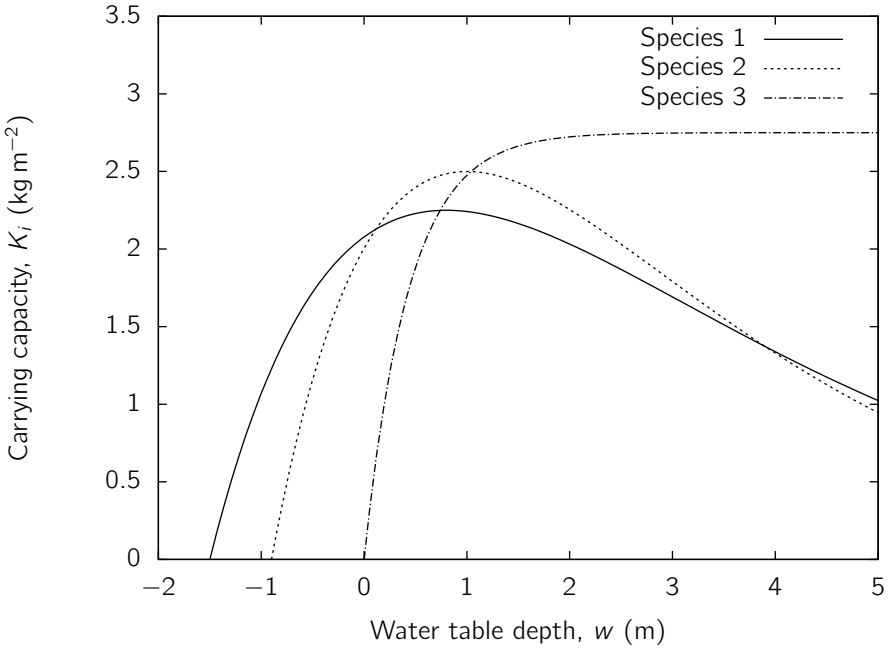

Figure 3.3: Carrying capacity curves for species 1 (flood tolerant wetland species), species 2 (less flood tolerant wetland species), and species 3 (dryland species).

For the wetland species, carrying capacity, K_1 and K_2 [ML^{-2}], were given by

$$K_i = K_i^\star \left(\frac{w - w_{ci}}{w_{pi} - w_{ci}} \right) \exp \left[\frac{w_{pi} - w}{w_{pi} - w_{ci}} \right] \tag{3.13}$$

where $K_i^\star$ [ML^{-2}] denotes maximum ecosystem carrying capacity of species i; w_{ci} [L] denotes a critical water table depth, below which, species i can no longer exist due to flooding stress (w_{ci} is usually negative to represent flooding); and w_{pi} [L] denotes the optimal water table depth, at which $K_i = K_i^\star$.

For the dryland species, carrying capacity, K_3 [ML^{-2}], was given by

$$K_3 = K_3^\star \left[1 - \exp \left(\frac{w - w_{c3}}{w_{p3} - w_{c3}} \ln 0.01 \right) \right] \tag{3.14}$$

where $K_3^\star$ [ML^{-2}] denotes maximum ecosystem carrying capacity of species 3; w_{c3} [L] denotes a critical water table depth, below which the carrying capacity of species 3 becomes zero because of waterlogging stress (usually positive); and w_{p3} [L] denotes the optimal water table depth, at which $K_3 = 0.99 K_3^\star \approx K_3^\star$.

3.5 Coupling Relationships

3.5.1 Evapotranspiration from the phreatic zone

Total evpotranspiration per unit land area from the phreatic zone, q_{Ts} [LT^{-1}], was given by the sum of evapotranspiration per unit land area from the phreatic zone for all vegetation species, i.e.

$$q_{Ts} = q_{Ts1} + q_{Ts2} + q_{Ts3} \tag{3.15}$$

Evapotranspiration per unit land area from the phreatic zone for species i, q_{Tsi} [LT^{-1}], was determined using the relationships found in Muneepeerakul et al. (2008). It was given by

$$q_{Tsi} = c_i(1 - R_i)B_i\frac{q_{Tmi}}{K_i^\star} \tag{3.16}$$

where c_i [$-$] is the anoxic stress coefficient of species i, reflecting reduced evapotranspiration under anoxic stress, due to roots being waterlogged; R_i [$-$] denotes the proportion of roots above the water table; and q_{Tmi} [LT^{-1}] is the maximum potential evapotranspiration per unit land area of species i—achieved when species i is at the maximum carrying system capacity, $K_i^\star$, and suffers neither anoxic stress due to waterlogging nor water stress due to soil dryness.

Proportion of roots above water table. Roots were taken to be exponentially distributed with mean depth R_{mi} [L], as was done in Muneepeerakul et al. (2008). The proportion of roots above the water table, R_i, was thus given by

$$R_i = \begin{cases} 0, & w \leq 0, \\ 1 - \exp\left(-\dfrac{w}{R_{mi}}\right), & w > 0. \end{cases} \tag{3.17}$$

3.5.2 Evapotranspiration from the vadose zone

Total evpotranspiration per unit land area from the vadose zone, q_{Tuns} [LT^{-1}], was given by the sum of evapotranspiration per unit land area from the vadose zone for all vegetation species, i.e.

$$q_{Tuns} = q_{Tuns1} + q_{Tuns2} + q_{Tuns3} \tag{3.18}$$

Evapotranspiration per unit land area from the vadose zone for species i, q_{Tunsi} [LT^{-1}], was determined using the relationships found in Muneepeerakul et al. (2008). It was given by

$$q_{Tunsi} = \rho_i R_i B_i \frac{q_{Tmi}}{K_i^\star} \tag{3.19}$$

where ρ_i [$-$] represents the plant water stress due to soil dryness of species i.

3.5.3 Plant water stress

Plant water stress of species i due to soil dryness, ρ_i [$-$], was modeled using the relationship found in Muneepeerakul et al. (2008). Plant water stress due to soil dryness set in when relative soil moisture of the vadose zone, S, dropped below a certain threshold value. The relationship was structured such that high plant water stress corresponded to a low value of ρ_i, and vice versa. ρ_i was given by

$$\rho_i = \begin{cases} 0, & 0 \leq S \leq S_{wi}, \\ \dfrac{S - S_{wi}}{S_i^\star - S_{wi}}, & S_{wi} < S < S_i^\star, \\ 1, & S \geq S_i^\star, \end{cases} \tag{3.20}$$

where S_{wi} [$-$] represents the relative soil saturation at which stomatal closure is fully completed for species i; and $S_i^\star$ [$-$] represents the relative soil saturation at which stomatal closure first begins for species i.

3.6 Model Parameters

Plant parameters. The plant parameters used in the model are given in Table 3.1. Parameters for species 1 (flood resistent wetland species) and species 2 (less flood resistent wetland species) were largely taken from Muneepeerakul et al. (2008). Parameters for species 3 (dryland species) were chosen to contrast with the other two species.

Table 3.1: Plant parameters used in the model. Parameters for species 1 (flood resistant) and species 2 (less flood resistant) were modified from those found in Muneepeerakul et al. (2008). Parameters for species 3 (dryland) were set to differentiate it from species 1 and 2.

			Species		
Parameter		Unit	1	2	3
α_{1j}	impact coefficient of species j on species 1	–	1	0.9	0.9
α_{2j}	impact coefficient of species j on species 2	–	0.9	1	0.9
α_{3j}	impact coefficient of species j on species 3	–	0.9	0.9	1
β_i	decay rate per unit biomass	$10^{-9}\,\mathrm{s}^{-1}$	68.29	71.47	71.47
ω_i	intrinsic water use efficiency	$\mathrm{kg\,m}^{-3}$	20.25	23.62	23.62
$K_i^\star$	maximum ecosystem carrying capacity	$\mathrm{kg\,m}^{-2}$	2.25	2.5	2.75
w_{ci}	critical water table depth	m	−1.5	−0.9	0
w_{pi}	optimal water table depth	m	0.8	1	2
q_{Tmi}	maximum potential evapotranspiration per unit land area	$10^{-9}\,\mathrm{m\,s}^{-1}$	57.87	57.87	57.87
R_{mi}	mean root depth	m	0.45	0.55	0.65
S_{wi}	relative soil saturation at which stomatal closure is fully completed	–	0.1177	0.1177	0.1177
$S_i^\star$	relative soil saturation at which stomatal closure first begins	–	0.2732	0.2732	0.2732
c_i	anoxic stress coefiicient	–	0.8	0.6	0.4
$initB_i$	initial value for biomass per unit land area	$\mathrm{kg\,m}^{-2}$	1.44	1.2	1

Soil and rainfall parameters. The soil and rainfall parameters used in the model are given in Table 3.2. Soil parameters were obtained from prior borehole investigations performed in areas surrounding the Nee Soon Wetland. Rainfall parameters were

derived from weather statistics published in National Environment Agency, Singapore (2011).

Table 3.2: Soil and rainfall parameters used in the model. Soil parameters were obtained from prior studies performed with the Nee Soon Wetland itself. Rainfall parameters were derived from weather statistics published in National Environment Agency, Singapore (2011).

Parameter		Unit	Value
K_s	soil saturated hydraulic conductivity	$10^{-6}\,\mathrm{m\,s^{-1}}$	7.93
η	soil porosity	–	0.44
N	exflitration calibration factor	$10^{-6}\,\mathrm{s^{-1}}$	1.16 to 11.6
S_{fc}	relative soil saturation at field capacity	–	0.32
E_{bot}	elevation of the level impermeable layer	m	-50
p	probability of a rainfall event on any single day	–	0.5
μ	mean amount of rainfall during a rainfall event	m	0.013

Chapter 4

Results and Discussion

Modeling was performed under both transient conditions (varying rainfall) and pseudo-stationary conditions (constant rainfall). Results from pseudo-stationary modeling served as a baseline against which results from transient modeling could be compared against. This chapter presents results obtained from both pseudo-stationary and transient modeling, and discusses the results obtained, regarding their significance towards the Nee Soon Wetland and their implications for future work.

4.1 Equation Input Verification

Equations input into the model were verified by performing a mass balance convergence study on a greatly simplified domain. Figure 4.1 shows the greatly simplified domain, which was a 15 km by 15 km square containing two square reservoirs, one upstream and one downstream. The same set of equations as the actual model was used, albeit without differentiation of land-use classes. All boundaries were set to no-flow, except those of the upper left box (representing an upstream reservoir), which were given Dirichlet boundary conditions for groundwater head. Characteristics of the meshes used are shown in Table 4.1, and results of the mass balance calculations are shown in Table 4.2 and Table 4.3.

The mass balances in the simplified model became more accurate when meshes

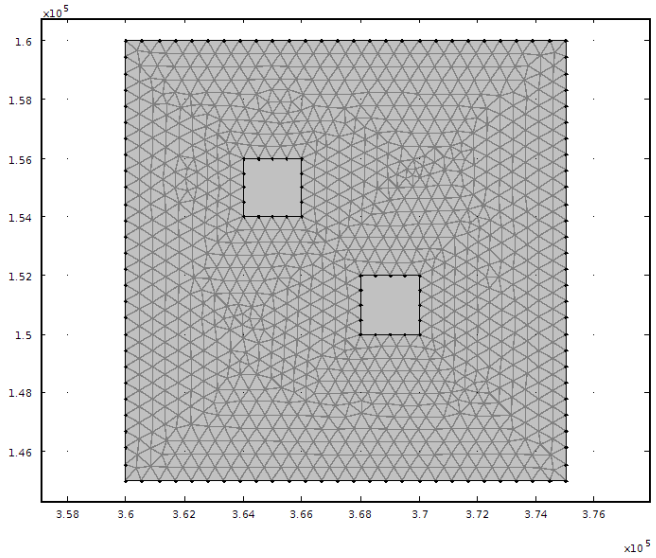

Figure 4.1: Greatly simplified domain used to verify if equations in the model were input correctly and if they fulfilled a mass balance. The upper left box represented an upstream reservoir and was assigned Dirichlet boundary conditions for groundwater head. All other model boundaries were set to no-flow.

Table 4.1: Characteristics of the meshes used in the greatly simplified domain.

Mesh	Element Size (m)		Max. Element Growth Rate (−)	Resolution of Curvature (−)
	Max.	Min.		
normal	1010	4.50	1.30	0.30
finer	555	1.88	1.25	0.25
extremely fine	150	0.30	1.10	0.20

Table 4.2: Results of stationary mass balance calculations for the simplified domain. Calculations were more accurate in meshes of finer resolution. All units in $m^3\,s^{-1}$.

Mesh	Evapotranspiration	Exfiltration	Inflow	Sum (should $\rightarrow$ 0)
normal	-0.202	-0.183	0.216	-0.168
finer	-0.205	-0.154	0.273	-0.086
extremely fine	-0.200	-0.150	0.332	-0.018

Table 4.3: Results of time-dependent mass balance calculations for the simplified domain. Calculations were more accurate in meshes of finer resolution.

Mesh	Average absolute error between volume change and sum of fluxes from all time steps ($m^3\,s^{-1}$)
normal	0.090
finer	0.043
extremely fine	0.022

of finer resolution were used. This strongly signalled that the equations were input into the model correctly, and that they were physically feasible from the point of view of a mass balance.

4.2 Pseudo-Stationary Modeling

Pseudo-stationary modeling was performed by setting raindrop arrival rate, Ra, to a constant value over the entire model run. The value of Ra was set such that yearly rainfall in the model equaled average yearly rainfall in Singapore. Pseudo-stationary simulations were run for one year, beyond which, the rate of change in vegetation patterning and hydrological conditions became very slow. The results obtained formed a basis for comparison with results from transient modeling.

The results show the close link between groundwater head, H, and ground elevation, E_{grd}, indicating that groundwater flow is primarily driven from areas of higher elevation to areas of lower elevation. Bukit Timah Hill, the southwest area of high elevation and high head in Figures 4.2(a) and 4.2(b), is a significant driver of groundwater flow, towards the Nee Soon Wetland. From the Nee Soon Wetland, groundwater flows northeast into the Lower Seletar Reservoir, which is situated at a lower elevation.

Zooming in closer into the Nee Soon Wetland, there is a sharp change in the water table elevation, w, from about 2 m to 5 m and more, seeming to provide a fairly clear delineation of the extents of the wetland boundaries (see Figure 4.2(c)). The value of w in most parts of the wetland is below 0.75 m, indicating that plants within the wetland are likely to encounter a significant amount of anoxic stress, as their mean root depth, R_{mi}, ranges from 0.45 m to 0.65 m (see Table 3.1). Relative soil saturation of the vadose zone, S, is relatively constant within the wetland, hovering close to relative soil saturation at field capacity, $S_{fc} = 0.32$. This suggests that plants both within and outside the wetland are unlikely to suffer from plant water stress due to soil dryness.

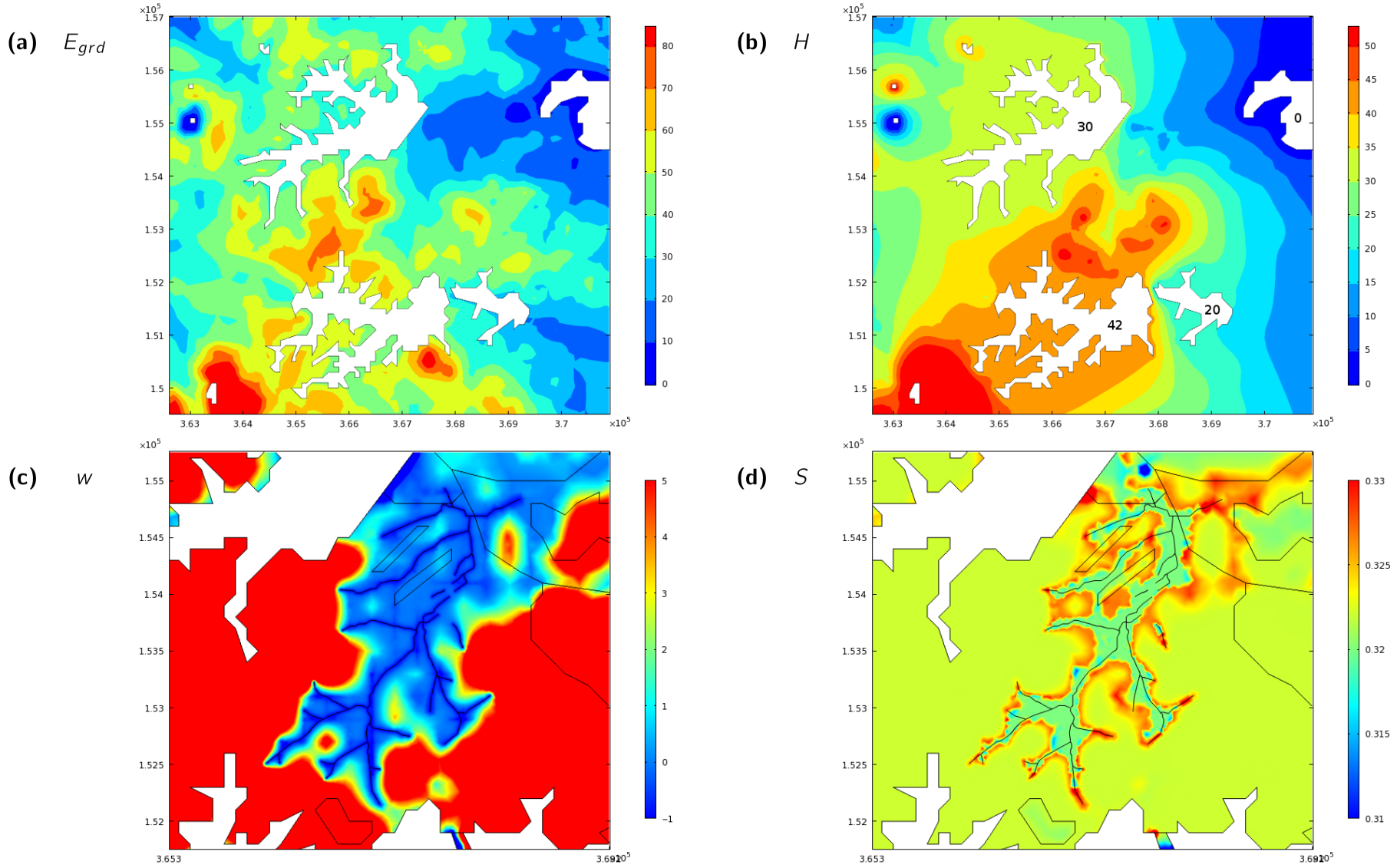

Figure 4.2: Results from pseudo-stationary modeling: (a) ground elevation, E_{grd} (m); (b) depth averaged groundwater head, H (m), where values inside reservoirs indicate values of H at reservoir Dirichlet boundaries; (c) water table depth, w (m); (d) relative soil saturation of vadose zone, S (−).

The distribution and coexistence of the three species of vegetation are shown in Figure 4.3. Within the Nee Soon Wetland, the results show the flood resistant species, species 1, having the upper hand, and completely outcompeting both the other species in regions within 100 m from the streams boundaries. The less flood resistant species, species 2, thrives on the fringes of the Nee Soon Wetland, especially in the region of the sharp change in w. The dryland species, species 3, is almost completely unable to exist within the wetland, but outcompetes both the other two species outside the wetland.

4.3 Transient Modeling

Transient modeling was performed over a time period of one year, using the stochastically generated rainfall pattern shown in Figure 4.4. The rainfall pattern was generated as a binomial process, with each day representing one binomial event.

Under transient modeling, variability in rainfall lead to quick and frequent changes in relative soil saturation of the vadose zone, S. During relatively dry periods (such as during the 5th month in Figure 4.4), the value of S dropped considerably below the value at which stomatal closure first begins, $S_i^\star = 0.2732$, over large extents of land area (see Figure 4.5). As a consequence, plant water stress due to soil dryness, ρ_i, which set in when $S < S_i^\star$ (see Equation 3.20), was prevalent during relatively dry periods.

To show the impact of variability in rainfall on ρ_i in more detail, plots of ρ_1 at different points in time are given in Figure 4.6. Note that for the same value of S, the parameter values chosen resulted in $\rho_1 = \rho_2 = \rho_3$ (see Equation 3.20 and Table 3.1). During relatively dry periods (eg. 5th month), the fringes of the wetland (where the less flood resistant wetland species thrives), and areas outside the wetland (where the dryland species thrives), experienced high plant water stress, i.e. $\rho_i < 0.5$. During periods of normal rainfall (eg. 3rd month), large portions of the these areas experienced considerable plant water stress, i.e. $\rho_i < 0.7$. Even during

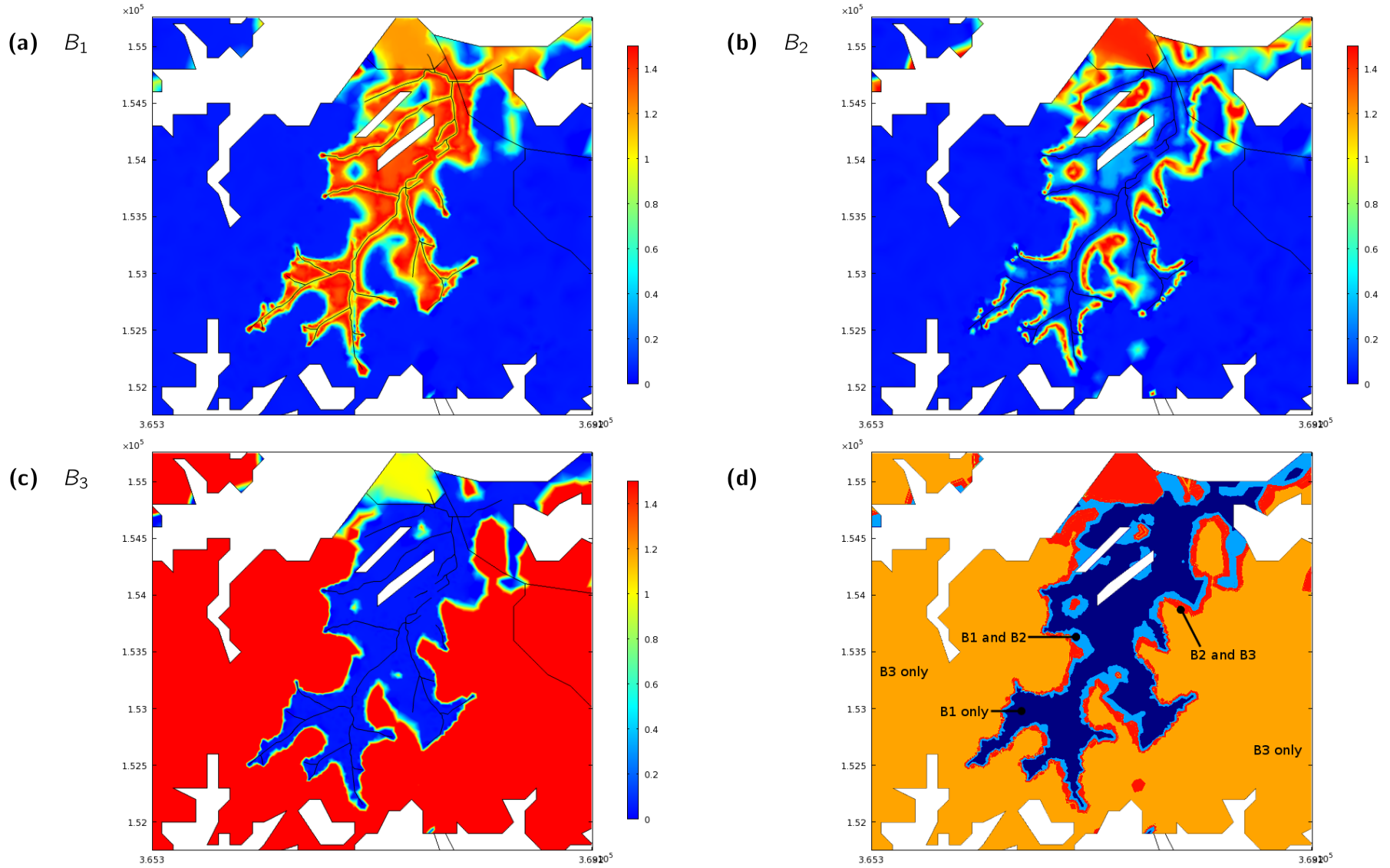

Figure 4.3: Results from pseudo-stationary modeling: (a) biomass density of flood resistant species, B_1 ($\mathrm{kg\,m^{-2}}$); (b) biomass density of less flood resistant species, B_2 ($\mathrm{kg\,m^{-2}}$); (c) biomass density of dryland species, B_3 ($\mathrm{kg\,m^{-2}}$); (d) species distribution and coexistence (shows regions where $B_i > 0.5\,\mathrm{kg\,m^{-2}}$).

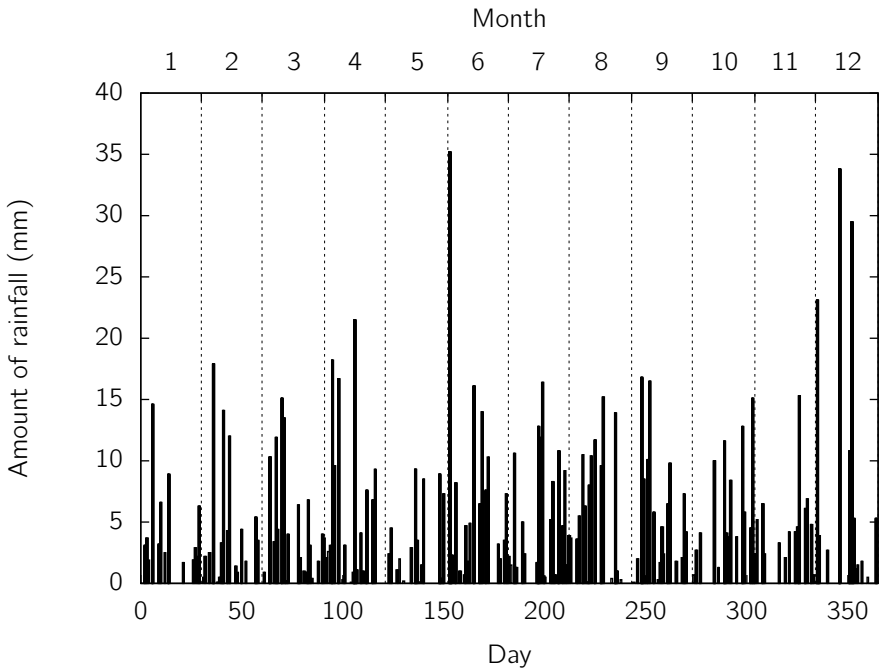

Figure 4.4: Typical realised values for amount of rainfall, shown here for a period of one year.

wetter periods (eg. 4th and 6th months), several areas still experienced $\rho_i < 0.8$. Comparing the above results to the rainfall pattern, shown in Figure 4.4, it becomes apparent that just a few days of low to zero rainfall can result in considerable plant water stress over several areas. Transient simulations are thus likely to be essential in adequately modeling the coupled hydrological-vegetation dynamics of the Nee Soon Wetland, due to the significant impact of rainfall variability on S, and by consequence on ρ_i as well.

Distribution and coexistence of the three species was significantly changed under transient modeling, as compared to under pseudo-stationary modeling (compare Figures 4.7(a) and 4.7(b)). Coexistence of both the flood resistant species, species 1, and the less flood resistance species, species 2, occurred over a much larger area. The area dominated by the dryland species, species 3, was significantly reduced. The results seem encouraging for the future of the wetland, as the two wetland species seem able to outcompete the dryland species over a larger area. This effect was not readily apparent from the beginning. However, a greater number of simulations, over longer time periods and under different rainfall patterns, are required to understand

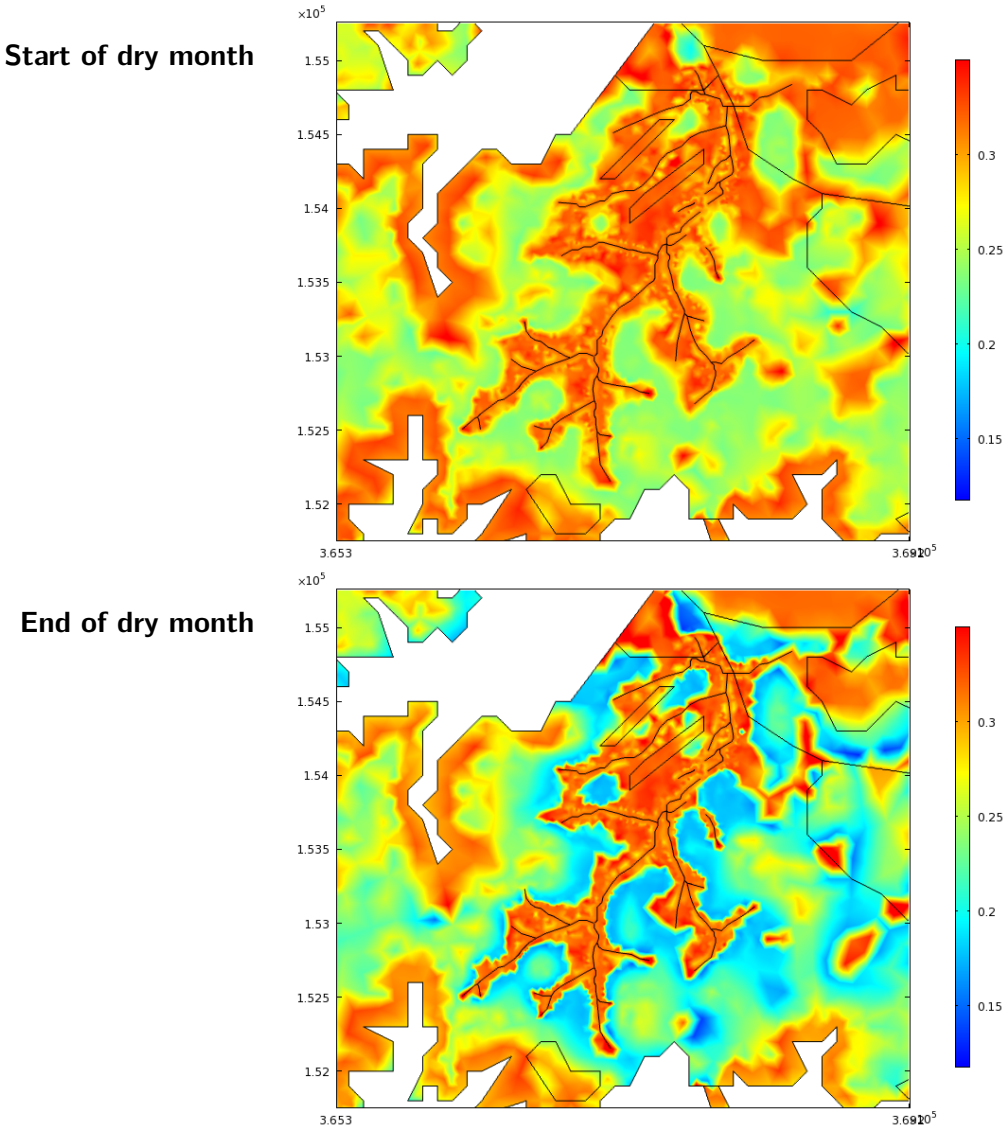

Figure 4.5: Results for relative soil saturation of the vadose zone, S, at the start and end of a relatively dry month (5th month in Figure 4.4). During the dry month, values of S dropped considerably below the value at which stomatal closure first begins, $S_i^\star = 0.2732$, over large areas.

the distribution and coexistence characteristics better.

The distribution and coexistence characteristics do however show that a clear delineation of the wetland is not possible using groundwater levels alone. Areas occupied by the two wetland and one dryland species are likely to pulsate with changes in rainfall pattern, albeit in a complex manner, with effects visible only after significant time delays. This is significant for legal protection of the Nee Soon Wetland, in which wetland delineation is likely to play a significant role.

Groundwater water head, H, and by extension, water table depth, w, were not as

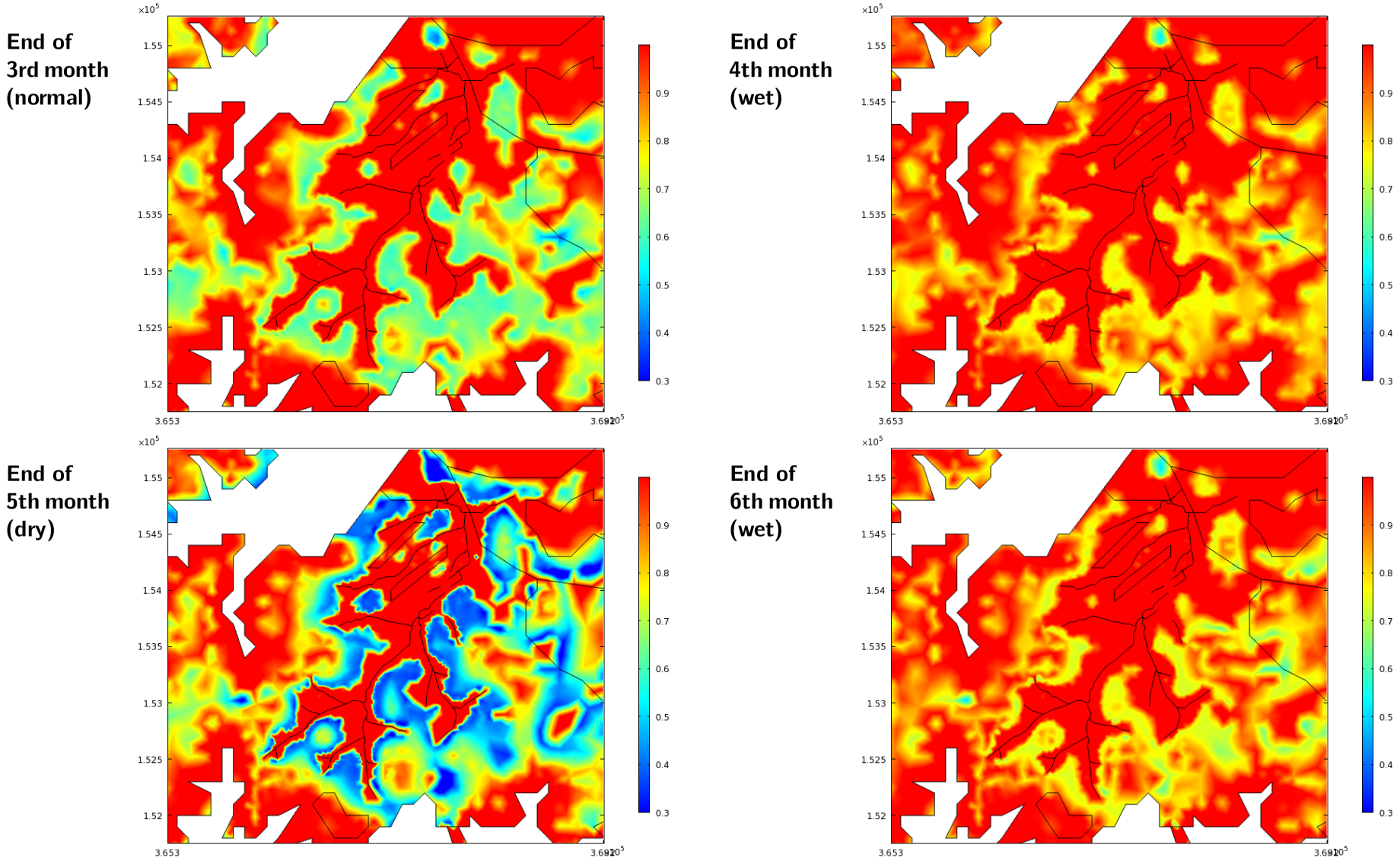

Figure 4.6: Results for plant water stress due to soil dryness of species 1, ρ_1, from a transient modeling run with the rainfall pattern given in Figure 4.4. Note that parameter values chosen resulted in $\rho_1 = \rho_2 = \rho_3$, and that a lower value for ρ_i indicates a higher plant water stress. Changes in ρ_i are sensitive to rainfall pattern, especially during dry periods.

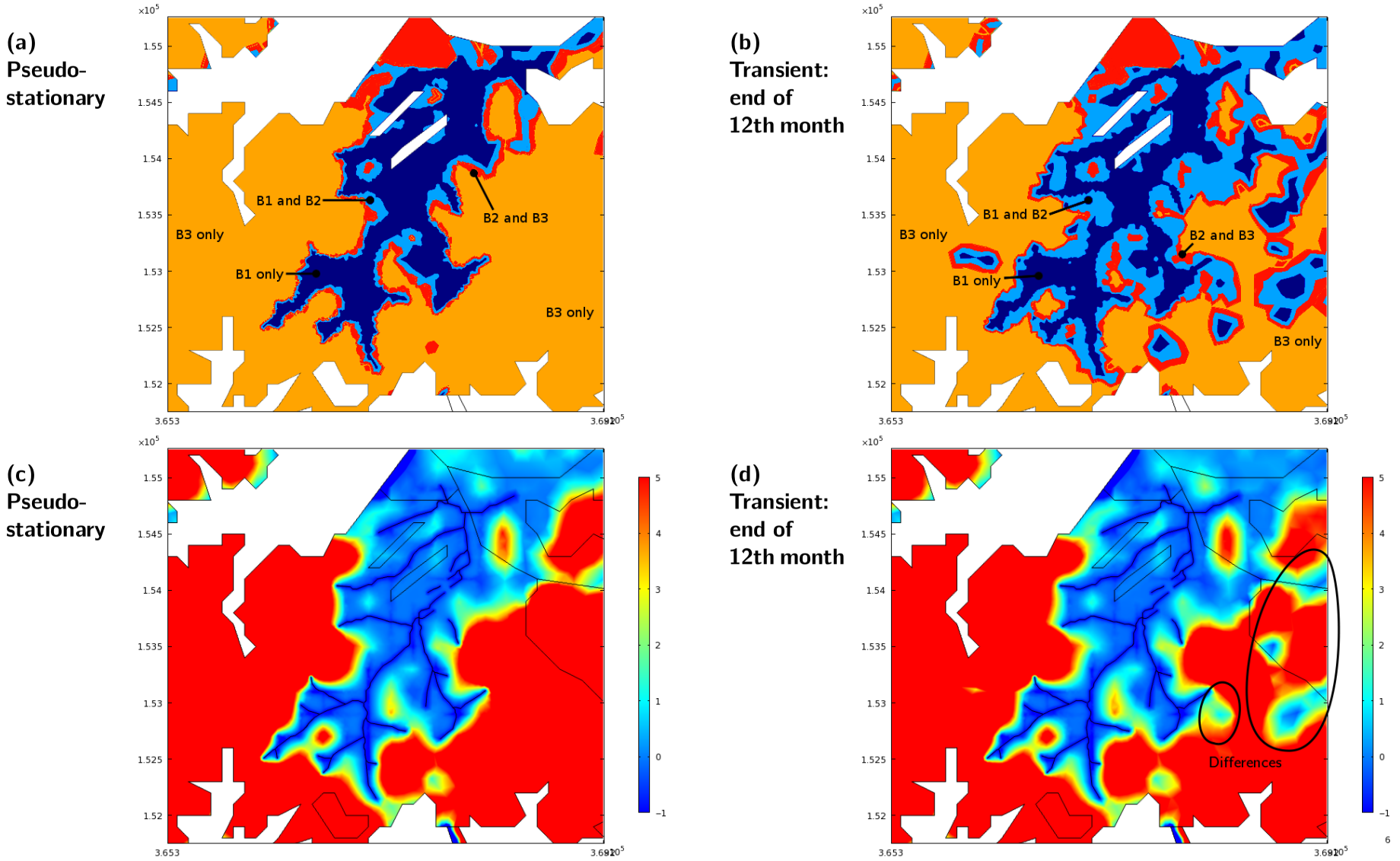

Figure 4.7: Comparison of results for species distribution and coexistence (plots show regions where $B_i > 0.5\,\mathrm{kg\,m^{-2}}$) and water-table depth, w (m), from pseudo-stationary modeling and transient modeling (end of 12th month): (a) species distribution and coexistence (pseudo-stationary); (b) species distribution and coexistence (transient); (c) w (pseudo-stationary); (d) w (transient).

sensitive to variations in rainfall as S, but differences between the pseudo-stationary and transient models could be seen within a period of one year. Figures 4.7(c) and 4.7(d) highlight some differences in the values of w, between the pseudo-stationary and transient models, at the end of a modeling period of 12 months. The lower sensitivity of H and w, to variations in rainfall, reaffirm previous findings that changes in S have a strong influence on vegetation dynamics. Modeling S, and other dynamics of the vadose zone, using a more sophisticated approach may thus be a prudent improvement to the current model.

Additionally, it is noted that H and w may have been strongly modulated by the fixed Dirichlet boundary conditions at stream locations within the wetland. Sensitivity studies, using different boundary conditions at stream locations, may indicate that an improved representation of streams, and possibly overland flow, is necessary.

4.4 Limitations and Future Work

The model currently lacks field data, especially for plant species parameters. Field data is important for model calibration and quantitative model verification. Future work will involve retrieving better estimates for vegetation parameters, from literature sources. Field data collection is also required, and the model, as it currently stands, can help prioritise field data collection efforts through sensitivity studies of model parameters.

Accounting for second order quantities, such as groundwater flows (derivative of groundwater head), is still an issue. For instance, within the course of the final year project, it was not possible to completely account for global mass balance in the model, probably due to difficulties in calculating for groundwater flux at the boundaries. The model was thus verified using a simplified domain, with the majority of boundaries being set to no-flow. Using a finer mesh improves accounting for the second order quantities, but results in much a much larger computational effort and memory usage requirements. The increased requirements when using a finer meshes

prevent the model from being solved on a personal computer—which is undesirable for practical model usage. An improved method of accounting for boundary flux, such as that found in Lynch (1984), is an possible area of future work.

The model currently uses a simplified method of coupling between the phreatic and vadose zones. The coupling currently involves linking specific yield, s_y, to relative soil saturation of the vadose, S, using a simple relation: $s_y = 1 - S$. The relation satisfies mass balance, and is valid when the groundwater table rises. However, it does not meet the definition of specific yield when the groundwater table falls. Additionally, results from transient modeling indicate a strong sensitivity of S to rainfall variations, and a strong impact of changes in S on vegetation dynamics. Thus, an improved method of modeling the vadose zone, and coupling the vadose and phreatic zones, is an area for future work. The coupling methodology found in Downer (2007) is one option for such an improvement.

As was discussed in Section 4.3, a greater number of simulations, over longer time periods, and under different rainfall conditions, are required to understand the impacts of rainfall pattern on the distribution and coexistence characteristics of the three vegetation species better. Also, sensitivity studies using different boundary conditions at stream locations within the wetland, may indicate that an improved representation of streams, and possibly overland flow, is necessary.

Chapter 5

Conclusions

A finite element coupled hydrological-vegetation model was developed for the Nee Soon Wetland. The model provided an approximately georeferenced two-dimensional (2D) aerial representation of the wetland and the hydrological-vegetation interactions within it. It modeled groundwater dynamics of both the phreatic and vadose zones, and biomass dynamics of three species of vegetation—a flood resistant wetland species, a less flood resistant wetland species and a dryland species. Dynamics of the phreatic zone was modeled using the standard groundwater equations for a 2D unconfined aquifer. Dynamics of the phreatic zone was modeled as a mass balance at a point. Biomass dynamics of the three vegetation species was modeled as a three species competitive Lotka-Volterra system.

The model included elevation data from the SRTM digital elevation model, locations of reservoirs, lakes and streams within and around the Nee Soon Wetland, and differentiated between vegetated areas, golf courses and built up areas. Rainfall was stochastically generated as a binomial process on the daily scale using local weather statistics.

Modeling was performed under both pseudo-stationary conditions (constant rainfall) and transient conditions (varying rainfall). Results from pseudo-stationary modeling served as a baseline against which results from transient modeling could be compared against. Results from transient modeling indicated that variations in

rainfall impacted plant water stress due to soil dryness, quickly and significantly. A dry period of one month was sufficient to induce considerable plant water stress along the fringes of the Nee Soon Wetland, and in areas outside the wetland. Through comparison with results from pseudo-stationary modeling, it was observed that areas occupied by the two wetland and one dryland species were likely to pulsate with changes in rainfall pattern, though in a complex manner, with effects visible only after significant time delays. This meant that a clear delineation of the wetland was unlikely, and that a greater number of simulations, using different rainfall patterns, and over longer time periods, were required to understand this phenomenon better.

The results also showed that the vadose zone dynamics (represented by relative soil saturation) were much more sensitive to variations in rainfall than the phreatic zone dynamics (represented by groundwater head and water table depth). Because of this, and because the model currently uses a simplified means of coupling the vadose and phreatic zones, it was concluded that a more sophisticated approach for modeling the vadose zone would be a prudent improvement. Additionally, it was noted that the phreatic zone dynamics may have been strongly modulated by the fixed Dirichlet boundary conditions for groundwater head at stream locations within the wetland. Thus, sensitivity studies may indicate that an improved representation of stream boundaries, and possibly overland flow, is necessary.

Future work would also involve improving vegetation parameter estimates, through literature review, field study and sensitivity analysis. This would allow for improved model calibration and quantitative model verification. Improvement to the methods used in accounting for second order quantities, such as groundwater flows (derivative of groundwater head), especially on model boundaries, are also required. This will allow the global mass balance to be solved for more accurately, and reduce computational and memory requirements for numerical solution.

Bibliography

Barbour, S. Lee and John Krahn (2004). "Numerical Modeling—Prediction or Process?" In: *Geotechnical News* 22, pp. 44–52.

Brady, Nyle C. and Ray R. Weil (2008). "Soil Water: Characteristics and Behaviour". In: *The Nature and Properties of Soils*. 14th Edition. Chap. 5.

COMSOL AB. (2010). *COMSOL Multiphysics*. Software. URL: http://www.comsol.com.

Cronk, Julie K. and M. Siobhan Fennessy (2001). "Adaptations to Growth Conditions in Wetlands". In: *Wetland Plants: Biology and Ecology*. CRC Press. Chap. 4.

Downer, Charles W. (2007). *Development of a Simple Soil Moisture Model in the Hydrologic Simulator GSSHA*. Technical Note ERDC TN-SWWRP-07-8. U.S. Army Engineer Research and Development Center. URL: https://swwrp.usace.army.mil/_swwrp/swwrp/4-Pubs/TechNotes/SWWRP-tn-07-8.pdf.

Farkas, Miklos (2001). "Population Dynamics in Continuous Time". In: *Dynamical Models in Biology*. Chap. 2.

GRASS Development Team (2008). *Geographic Resources Analysis Support System (GRASS GIS)*. Open Source Geospatial Foundation. Software. URL: http://grass.osgeo.org.

Hannah, David M., Paul J. Wood, and Jonathan P. Sadler (2004). "Ecohydrology and hydroecology: A 'new paradigm'?" In: *Hydrological Processes* 18, pp. 3439–3445.

Hunt, Randall J. and Douglas A. Wilcox (2003). "Ecohydrology—Why Hydrologists Should Care". In: *Groundwater* 41 (3), p. 289.

Jarvis, A. et al. (2008). *Hole-filled seamless SRTM data V4*. International Centre for Tropical Agriculture (CIAT). Digital Elevation Model. URL: http://srtm.csi.cgiar.org.

Keddy, Paul A. (2000). *Wetland Ecology: Principles and Conservation*. Cambridge University Press.

Laio, F. et al. (2001). "Plants in water-controlled ecosystems: active role in hydrologic processes and response to water stress: II. Probabilistic soil moisture dynamics". In: *Advances in Water Resources* 24, pp. 707–723.

Lillesand, Thomas M., Ralph W. Kiefer, and Jonathan W. Chipman (2003). *Remote Sensing and Image Interpretation*. John Wiley & Sons.

Loheide II, Steven P. and Steven M. Gorelick (2007). "Riparian Hydroecology: A coupled model of the observed interactions between groundwater flow and meadow vegetation patterning". In: *Water Resources Research* 43, W07414.

Lynch, Daniel R. (1984). "Mass conservation in finite element groundwater models". In: *Advances in Water Resources* 7 (2), pp. 67–75.

Muneepeerakul, Chitsomanus P. et al. (2008). "Coupled hydrologic and vegetation dynamics in wetland ecosystems". In: *Water Resources Research* 44, W07421.

National Environment Agency, Singapore (2011). *Weather Statistics*. Accessed 01 January 2011. URL: http://app2.nea.gov.sg/weather_statistics.aspx.

Ng, Peter K. L. and Kevin K. P. Lim (1992). "The conservation status of the Nee Soon freshwater swamp forest of Singapore". In: *Aquatic Conservation: Marine and Freshwater Ecosystems* 2, pp. 255–266.

RibbonSoft GmbH (2008). *QCAD Community Edition*. Open Source Geospatial Foundation. Software. URL: http://www.qcad.org.

Richardson, J.L., J.L. Arndt, and J.A. Montgomery (2001). "Hydrology of Wetland and Related Soils". In: *Wetland Soils*. Ed. by M.J. Vepraskas and J.L. Richardson. Chap. 4.

Ridolfi, L., P. D'Odorico, and F. Laio (2006). "Effect of vegetation-water table feedbacks on the stability and resilience of plant ecosystems". In: *Water Resources Research* 43, W01201.

Rodriguez-Iturbe, I. et al. (1999). "Probabilistic Modelling of Water Balance at a Point: The Role of Climate, Soil and Vegetation". In: *Proceedings: Mathematical, Physical and Engineering Sciences*. Vol. 455 (1990). The Royal Society, pp. 3789–3805.

Rodriguez-Iturbe, I. et al. (2001). "Plants in water-controlled ecosystems: active role in hydrologic processes and response to water stress: I. Scope and general outline". In: *Advances in Water Resources* 24, pp. 695–705.

Wassen, Martin J. and Ab P. Grootjans (1996). "Ecohydrology: an interdisciplinary approach for wetland management and restoration". In: *Vegetatio* 126, pp. 1–4.